1521-0111/88/2/380–389$25.00
MOLECULAR PHARMACOLOGY

http://dx.doi.org/10.1124/mol.115.098012
Mol Pharmacol 88:380–389, August 2015

Pharmacologic Inhibition of MNKs in Acute Myeloid Leukemia

Theodosia Teo, Frankie Lam, Mingfeng Yu, Yuchao Yang, Sunita K. C. Basnet, Hugo Albrecht, Matthew J. Sykes, and Shudong Wang

Centre for Drug Discovery and Development, Sansom Institute for Health Research, Centre for Cancer Biology, and School of Pharmacy and Medical Sciences, University of South Australia, Adelaide, Australia

Received January 19, 2015; accepted June 4, 2015

ABSTRACT

The Ras/Raf/MAPK and PI3K/Akt/mTOR pathways are key signaling cascades involved in the regulation of cell proliferation and survival, and have been implicated in the pathogenesis of several types of cancers, including acute myeloid leukemia (AML). The oncogenic activity of eIF4E driven by the Mnk kinases is a convergent determinant of the two cascades, suggesting that targeting the Mnk/eIF4E axis may provide therapeutic opportunity for the treatment of cancer. Herein, a potent and selective Mnk2 inhibitor (MNKI-85) and a dual-specific Mnk1 and Mnk2 inhibitor (MNKI-19), both derived from a thienopyrimidinyl chemotype, were selected to explore their antileukemic properties. MNKI-19 and MNKI-85 are effective in inhibiting the growth of AML cells that possess an M5 subtype with FLT3-internal tandem duplication mutation. Further mechanistic studies show that the downstream effects with respect to the selective Mnk1/2 kinase inhibition in AML cells causes G_1 cell cycle arrest followed by induction of apoptosis. MNKI-19 and MNKI-85 demonstrate similar Mnk2 kinase activity and cellular antiproliferative activity but exhibit different time-dependent effects on cell cycle progression and apoptosis. Collectively, this study shows that pharmacologic inhibition of both Mnk1 and Mnk2 can result in a more pronounced cellular response than targeting Mnk2 alone. However, MNKI-85, a first-in-class inhibitor of Mnk2, can be used as a powerful pharmacologic tool in studying the Mnk2/eIF4E-mediated tumorigenic mechanism. In conclusion, this study provides a better understanding of the mechanism underlying the inhibition of AML cell growth by Mnk inhibitors and suggests their potential utility as a therapeutic agent for AML.

Introduction

Acute myeloid leukemia (AML) is a genetically heterogeneous cancer characterized by a collection of mutations and chromosomal translocations in immature myeloid cells that cooperate to interrupt the proliferative or survival pathways (Gilliland et al., 2004). The aberrant fusion transcription factors expressed in myeloid cells can impair hematopoietic differentiation; however, a single genetic alteration is insufficient to induce leukemogenesis in most cases (He et al., 1997; Yuan et al., 2001). Particularly, constitutively activated signal transduction pathways derived from the mutated genes that normally regulate hematopoietic cell growth and homeostasis are additional contributors to the pathogenesis of AML (Dash and Gilliland, 2001).

The Ras/Raf/MAPK and PI3K/Akt/mTOR signaling pathways are two vital cascades that are physiologically relevant to diverse cell stimuli involved in differentiation, proliferation, and apoptosis (Lewis et al., 1998; Hanada et al., 2004). Activation of these pathways has been associated with most AML cases (Milella et al., 2001; Martelli et al., 2006). Another common molecular defect, FLT3 mutation, is highly expressed in AML, accounting for 70–100% of all cases (Gilliland and Griffin, 2002). Specifically, the presence of internal tandem duplication (ITDs) in the juxtamembrane domain of FLT3 was found in nearly one-third of patients with AML and is associated with a poor prognosis (Meshinchi et al., 2001). Therefore, these signal transduction cascades may represent promising areas to exploit with therapeutic intent in AML.

Interestingly, the aforementioned cascades consequently converge on the Mnks/eIF4E axis, which plays a significant regulatory role in mRNA translation and malignant transformation. The phosphorylation of eIF4E by Mnk at Ser209 has been implicated in tumorigenesis and development (Waskiewicz et al., 1997; Furic et al., 2010). While Mnk activity is not essential for normal cell growth (Ueda et al., 2004), the oncogenic activity of Mnk-driven eIF4E has been shown to be vital for the proliferation and survival of cancer cells (Topisirovic et al., 2004; Wendel et al., 2007). Therefore, therapeutic targeting of Mnk offers an opportunity in the treatment of cancer.

Mnks belong to a serine/threonine kinases family, and were identified as unique interacting proteins for ERK and p38 kinases in the MAPK cascade (Waskiewicz et al., 1997; Roux and Blenis, 2004). Two Mnk human genes have been identified, expressing Mnk1 and Mnk2 proteins that are ~72% identical in

This work was supported by the Australian Government National Health and Medical Research Council [Grant 1050825], and the Beat Cancer Project Principal Cancer Research Fellowship by South Australian Health and Medical Research Institute to S.W.
dx.doi.org/10.1124/mol.115.098012.
This article has supplemental material available at molpharm.aspetjournals.org.

ABBREVIATIONS: AML, acute myeloid leukemia; CGP57380, N^3-(4-fluorophenyl)-1*H*-pyrazolo-[3,4-*d*]pyrimidine-3,4-diamine; DCM, dichloromethane; DMSO, dimethylsulfoxide; FA, formic acid; ITD, internal tandem duplications; MNKI-19, 4-((4-fluoro-2-isopropoxyphenyl)amino)-5-methylthieno[2,3-*d*]pyrimidine-6-carboxylic acid; MNKI-85, 4-((4-fluoro-2-isopropoxyphenyl)amino)-*N*-(2-methoxyethyl)-5-methylthieno[2,3-*d*]pyrimidine-6-carboxamide; PI, propidium iodide; RP-HPLC, reversed-phase high-performance liquid chromatography; WT, wild-type.

their amino acid sequence (Slentz-Kesler et al., 2000). Alternative splicing in the two Mnk genes further revealed the existence of four isoforms: *Mnk1a*, *Mnk1b*, *Mnk2a*, and *Mnk2b* (Waskiewicz et al., 1997; Scheper et al., 2003). Bearing a nuclear localization signal and a polybasic sequence in the common basic N-terminal stretch, all four isoforms preferentially localize in the nucleus and phosphorylate eIF4E efficiently.

The difference between the four isoforms arises from the C termini, in which only the a-isoforms have a MAPK-binding site for interaction with ERK or p38 kinases (Parra et al., 2005). Despite this, Mnk1a and Mnk2a differ in basal activity as has been shown in in vitro studies (Scheper et al., 2001). Activation of ERK or p38 kinase could result in a marked increase in the activation of the low basal activity of Mnk1a, but would negligibly influence the high basal activity of Mnk2a. Both Mnk1a and Mnk2a bind preferentially to ERK but only Mnk1a is a substrate for p38. In appreciation of the dissimilarity in the regulatory features of Mnk1 and Mnk2, these findings may indicate differences in activity and regulation of Mnks toward eIF4G to phosphorylate eIF4E.

An increasing body of evidence has demonstrated the potential antileukemic properties of pharmacologic Mnk inhibitors (Altman et al., 2013; Lim et al., 2013; Diab et al., 2014b). Cercosporamide, a nonselective Mnk inhibitor (Konicek et al., 2011), reduces leukemic cell proliferation in MM6, K562, and U937 cell lines in a dose-dependent manner (Altman et al., 2013). The antitumor efficacy of cercosporamide in MV4-11 xenografts supports its Mnk-targeted antileukemic effects. The cell-specific effects, predominantly in leukemia cells, of Mnk inhibition have been recently confirmed by the recent discovery of 5-(2-(phenylamino)pyrimidin-4-yl)thiazole-2(*3H*)-one Mnk inhibitors (Diab et al., 2014b).

We have recently identified thieno[2,3-*d*]pyrimidine derivatives as highly potent and selective Mnk inhibitors. Herein, a potent dual-specific Mnk1/2 inhibitor (MNKI-19, 4-((4-fluoro-2-isopropoxyphenyl)amino)-5-methylthieno[2,3-*d*]pyrimidine-6-carboxylic acid) and a selective Mnk2 inhibitor (MNKI-85, 4-((4-fluoro-2-isopropoxyphenyl)amino)-*N*-(2-methoxyethyl)-5-methylthieno[2,3-*d*]pyrimidine-6-carboxamide) were used to provide mechanistic insights into the effects of Mnk isoforms on leukemia cells. Both MNKI-19 and MNK-85 are able to reduce the level of phosphorylated eIF4E and subsequently cause G_1 phase cell cycle arrest and apoptosis in FLT3-ITD–expressed AML cells. The current report also demonstrates that a combined inhibition of Mnk1 and Mnk2 results in a more pronounced cellular response than targeting Mnk2 alone, supporting the claim that Mnk inhibitors can be developed as potential anticancer agents.

Materials and Methods

Inhibitor Compounds and Proteins. Syntheses of MNKI-19 and MNKI-85 are described subsequently. The Mnk inhibitor N^3-(4-fluorophenyl)-1*H*-pyrazolo-[3,4-*d*]pyrimidine-3,4-diamine (CGP57380) was purchased from Sigma-Aldrich (Castle Hill, NSW, Australia), and used as a positive control. All compounds used were dissolved in dimethylsulfoxide (DMSO) at a stock concentration of 10 mM, and stored at −20°C in small aliquots. The eIF4E-derived peptides TAMRA-DTATKSGSTTKNR, TAMRA-DTATKSG(phospho)STTKNR, and DTATKSGSTTKNR were custom synthesized by Mimotopes Pty. Ltd. (Melbourne, VIC, Australia). Proteins Mnk1 and Mnk2 were purchased from Life Technologies (Grand Island, NY) and Merck Millipore (Billerica, MA), respectively.

Synthesis of MNKI-19 and MNKI-85. ^{1}H and ^{13}C NMR spectra were recorded at 298 K on an AVANCE III HD 500 spectrometer (Bruker, Faellanden, Switzerland) (^{1}H at 500.16 MHz and ^{13}C at 125.76 MHz), and were analyzed using the Topspin 3.2 software (Bruker). The ^{1}H and ^{13}C NMR spectra are referenced to ^{1}H signals of residual nondeuterated solvents and ^{13}C signals of deuterated solvents, respectively. The ^{1}H NMR signals are reported with chemical shift values δ (ppm), multiplicity (where s = singlet, d = doublet, t = triplet, dd = doublet of doublets, td = triplet of doublets, m = multiplet, and br = broad), relative integral, coupling constants J (Hz), and assignments. High-resolution mass spectra were recorded on a TripleTOF 5600 mass spectrometer (AB SCIEX, Concord, Ontario, Canada), and ionization of all samples was carried out using electrospray ionization. Melting points were determined using an open capillary on a Stuart SMP10 (Staffordshire, UK) melting point apparatus and were uncorrected. The purity of the compounds used for biologic evaluation was determined by analytic reversed-phase high-performance liquid chromatography (RP-HPLC), which was carried out on a Prominence UFLC System (Shimadzu, Kyoto, Japan) equipped with a CBM-20A communications bus module, a DGU-20A5R degassing unit, an LC-20AD liquid chromatograph pump, an SIL-20AHT auto-sampler, an SPD-M20A photo-diode array detector, a CTO-20A column oven and a Phenomenex Kinetex 5u C18 100A 250 mm × 4.60 mm column (Shimadzu). Method A [gradient 5–95% CH_3OH containing 0.1% formic acid (FA) over 7 minutes at a flow rate of 1 ml/min, followed by 95% CH_3OH containing 0.1% FA over 13 minutes] and method B (gradient 5–95% CH_3CN containing 0.1% FA over 7 minutes at a flow rate of 1 ml/min, followed by 95% CH_3CN containing 0.1% FA over 13 minutes) were used for the analytic RP-HPLC. Data acquired from the analytic RP-HPLC were processed using LabSolutions Analysis Data System (Shimadzu).

To a solution of methyl 4-((4-fluoro-2-isopropoxyphenyl)amino)-5-methylthieno[2,3-*d*]pyrimidine-6-carboxylate (200 mg, 0.533 mmol) in a mixture of THF/MeOH/H_2O (1:1:1, 60 ml), LiOH (382 mg, 16.0 mmol) was added. The reaction mixture was stirred at room temperature overnight and washed with dichloromethane (DCM) (20 ml). The aqueous layer was heated at 50°C for 10 minutes and acidified to pH 3 with 2 M HCl. The precipitate was filtered, washed with H_2O (3 × 25 ml), and dried under reduced pressure to give MNKI-19 as a white solid (128 mg, 67%), with R_F (DCM:MeOH = 9:1) 0.28; m.p. > 300°C; ^{1}H NMR (DMSO-d_6): δ 1.32 [d, 6H, J 6.0, OCH(CH_3)$_2$], 3.07 (s, 3H, thiophene-CH_3), 4.75–4.80 [m, 1H, OC*H*(CH_3)$_2$], 6.80 (td, 1H, J 8.5 and 2.5, benzene-H), 7.07 (dd, 1H, J 11.0 and 2.5, benzene-H), 8.47 (s, 1H, NH), 8.54 (s, 1H, pyrimidine-H), and 8.56 (dd, 1H, J 9.0 and 6.5, benzene-H) (one carboxylic acid proton signal not observed); ^{13}C NMR (DMSO-d_6): δ 15.3, 21.7, 71.5, 101.1 (d, $J_{C\text{-}F}$ 26.8), 106.1 (d, $J_{C\text{-}F}$ 21.6), 117.8, 121.9 (d, $J_{C\text{-}F}$ 9.4), 123.9, 125.0 (d, $J_{C\text{-}F}$ 2.6), 137.5, 148.3 (d, $J_{C\text{-}F}$ 10.6), 155.1, 156.1, 158.6 (d, $J_{C\text{-}F}$ 239.0), and 163.9, 166.3 (one carbon signal overlapping or obscured); high-resolution mass spectrometry (electrospray ionization) m/z 362.1500 $[M^+H]^+$; calculated for $C_{17}H_{17}FN_3O_3S^+$ 362.0969 $[M^+H]^+$; and analytic RP-HPLC method A: t_R 16.95 minutes, purity > 97% and method B: t_R 12.48 minutes, purity > 97%.

To a solution of 4-((4-fluoro-2-isopropoxyphenyl)amino)-5-methylthieno[2,3-*d*]pyrimidine-6-carboxylic acid (200 mg, 0.533 mmol) in *N*,*N*-dimethylformamide (3 ml), *N*,*N*-diisopropylethylamine (193 μl, 1.11 mmol) and *O*-(7-azabenzotriazol-1-yl)-*N*,*N*,*N*′,*N*′-tetramethyluronium hexafluorophosphate (316 mg, 0.830 mmol) were added. The reaction mixture was stirred in an ice bath for 30 minutes. Then, 2-methoxypropylamine (54.0 μl, 0.609 mmol) was added, and the reaction mixture was stirred at room temperature overnight and concentrated under reduced pressure. The residue was dissolved in DCM (20 ml), washed with saturated $NaHCO_3$ (3 × 20 ml), 10% citric acid (3 × 20 ml), H_2O (3 × 20 ml), and brine (3 × 20 ml), and concentrated under reduced pressure. The residue was purified by Biotage (Charlotte, NC) FlashMaster Personal$^+$ flash chromatography (silica gel, DCM ramping to DCM:EtOAc = 4:1) to give MNKI-85 as a white solid (118 mg, 51%), with R_F (DCM:EtOAc = 7:3) 0.54; m.p. 186–187°C; ^{1}H NMR ($CDCl_3$): δ 1.43 [d, 6H, J 6.0, OCH(CH_3)$_2$], 3.06 (s, 3H, thiophene-CH_3), 3.41 (s, 3H, OCH_3), 3.56–3.60 (m, 2H, CH_2CH_2O),

3.63–3.67 (m, 2H, CH_2CH_2O), 4.64–4.69 [m, 1H, $OCH(CH_3)_2$], 6.34 (br s, 1H, CONH), 6.69 (dd, 1H, *J* 10.0 and 3.0, benzene-H), 6.73 (td, 1H, *J* 8.5 & 2.5, benzene-H), 8.47 (br s, 1H, pyrimidine-NH-benzene), 8.61 (s, 1H, pyrimidine-H), and 8.77 (dd, 1H, *J* 9.0 and 6.5, benzene-H); ^{13}C NMR ($CDCl_3$): δ 16.1, 22.2, 40.1, 59.1, 70.3, 71.9, 100.5 (d, $J_{C\text{-}F}$ 27.0), 106.8 (d, $J_{C\text{-}F}$ 21.6), 118.3, 121.7 (d, $J_{C\text{-}F}$ 9.0), 124.9, 127.3, 132.9, 147.7 (d, $J_{C\text{-}F}$ 9.5), 154.2, 156.2, 159.1 (d, $J_{C\text{-}F}$ 241.5), and 162.9 (two carbon signals overlapping or obscured); high-resolution mass spectrometry (electrospray ionization) *m/z* 419.1394 $[M+H]^+$; calculated for $C_{20}H_{24}FN_4O_3S^+$ 419.1548 $[M+H]^+$; and analytic RP-HPLC method A: t_R 16.01 minutes, purity > 96% and method B: t_R 11.98 minutes, purity > 96%.

Cell Culture. All leukemia cell lines including HL-60, K562, MOLM-13, MV4-11, PL-21, THP-1, and U937 cells were kindly provided by Richard D'Andrea (University of South Australia, Adelaide, SA, Australia) and were maintained in Roswell Park Memorial Institute-1640 medium with 10% fetal bovine serum. The normal lung fibroblast cell line, WI-38, was obtained from the cell bank at the Centre for Drug Discovery and Development, University of South Australia, and was maintained in minimum essential media with 10% fetal bovine serum, 2 mM L-glutamine, and 1% nonessential amino acid. All cell lines were cultured in a humidified 37°C, 5% CO_2 incubator.

Kinase Assays. Inhibition of CDK2/cyclin A1, CDK9/cyclin T1, CDK4/cyclin D1, FLT3, Pim-1, B-Raf, MAPK1 (ERK2), MAPK2, PKBα (Akt1), PI3K (p110β/p85α), SAPK2α (p38α), and mTOR was measured by radiometric assays using the Millipore KinaseProfiler services with ATP concentrations within 15 μM of apparent K_m(app) for each kinase. For CDK2/cyclin A1, CDK9/cyclin T1, CDK4/cyclin D1, FLT3, and Pim-1 kinases, the IC_{50} values were calculated from 10-point dose-response curves and the apparent inhibition constants (K_i) were calculated from the IC_{50} values and appropriate ATP values using the Cheng and Prusoff (1973) equation. For the kinase panel screen, the kinase activities were reported as remaining activities that were calculated as percentage relative to the averages of multiplying the 0 and 100% controls, at a compound concentration of 5 μM.

Immobilized Metal Ion Affinity Particle Time-Resolved Fluorescence Energy Transfer Progressive Binding System. Each compound (1 and 10 μM in 0.5% DMSO) was added to the kinase reaction containing 1× immobilized metal ion affinity particle reaction buffer with Tween-20 dithiothreitol, distilled H_2O, TAMRA-labeled eIF4E peptide substrate, and Mnk kinase in a total assay volume of 20 μl. The kinase reaction was initiated by addition of ATP, incubated at 30°C for 90 minutes, and stopped with 60 μl progressive binding solution [30% binding buffer A, 70% binding buffer B, progressive binding reagent (1:600) and terbium donor (1:400)], followed by incubation in the dark at room temperature for 5 hours. After the incubation, the plate was read in an EnVision Multilabel Plate Reader (PerkinElmer, Beaconsfield, UK). The excitation wavelength for the terbium donor was set at 330 nm, while emissions were measured at 545 nm (terbium emission) and 572 nm (time-resolved fluorescence energy transfer emission) in a time-resolved manner with a delay of 200 microseconds. Positive and negative controls were performed in 0.5% DMSO in the presence and absence of Mnk kinases, respectively.

ADP-Glo Kinase Assay. The ADP-Glo assay kits were purchased from Promega (Madison, WI). Serial dilution of compounds with a dilution factor of 1:3 was performed to give eight concentrations ranging from 10 to 4.5 nM with 0.5% DMSO. Each compound was added to the kinase reaction containing 1× kinase reaction buffer, 0.1 mg/ml bovine serum albumin, distilled H_2O, eIF4E peptide substrate, and Mnk kinase in a total assay volume of 15 μl. The kinase reaction was initiated by addition of ATP, incubated at 30°C for 45 minutes, and stopped with 15 μl ADP Glo reagent, followed by incubation in the dark at room temperature for 40 minutes, and then 30 μl kinase detection reagent was added. The mixture was further incubated for 40 minutes before reading in the EnVision Multilabel Plate Reader (PerkinElmer). Positive and negative controls were performed with 0.5% DMSO in the presence and absence of Mnk kinases, respectively.

Cell Viability Assays. Resazurin (Sigma-Aldrich) and MTT (3-(4,5-dimethylthiazol-2-yl)-2,5-diphenyltetrazolium bromide) (Life Technologies, Mulgrave, VIC, Australia) assays were performed on all leukemia cell lines and normal lung fibroblast, respectively, as previously reported (Diab et al., 2014b). Compound concentrations required to inhibit 50% of cell growth (GI_{50}) were calculated using nonlinear regression analysis.

Caspase-3/7 Assay. The activity of caspase-3/7 was measured using the Apo-ONE Homogeneous Caspase-3/7 kit (Promega), according to the manufacturer's instructions, and analyzed using the EnVision Multilabel Plate Reader (PerkinElmer).

Cell Cycle and Detection of Apoptosis. MOLM-13 and MV4-11 (1×10^5) cells were seeded and incubated overnight at 37°C, 5% CO_2. Cells were centrifuged at 300*g* for 5 minutes upon treatment with each compound. Cell pellets were collected and fixed with 70% ethanol on ice for 15 minutes, followed by centrifugation at 300*g* for 5 minutes. The collected pellets were incubated with staining solution [50 μg/ml propidium iodide (PI), 0.1 mg/ml ribonuclease A, and 0.05% Triton X-100] at 37°C for 1 hour and analyzed with a Gallios flow cytometer (Beckman Coulter, Brea, CA). Then, 1×10^5 of the remaining cells were used for the apoptotic assay with the Annexin V-fluorescein Isothiocyanate Apoptosis Detection Kit (Becton Dickenson, Franklin Lakes, NJ), following the manufacturer's instructions. The samples were analyzed by fluorescence-activated cell sorting with the flow cytometer within 1 hour of staining. Data were analyzed using Kaluza v1.2 (Beckman Coulter).

Western Blots. Western blotting was performed as described previously (Wang et al., 2004). The antibodies used were as follows: Mnk2 and phosphorylated Rb at Thr821 (p-Rb^{T821}) (Abcam, Cambridge, UK), β-actin, caspase-3, CDK4, CDK6, cyclin D3, eIF4E, phosphorylated eIF4E at Ser209 (p-$eIF4E^{S209}$), 4E-BP1, phosphorylated 4E-BP1 at Thr37/46 (p-4E-$BP1^{T37/46}$) and Thr70 (p-4E-$BP1^{T70}$), phosphorylated p42/p44 at Thr202/Tyr204 (p-$ERK^{T202/Y204}$), Mcl-1, PARP, cleaved PARP, Mnk1, p38, phosphorylated p38 at Thr180/Tyr182 (p-$p38^{T180/Y182}$) (Cell Signaling Technologies, Danvers, MA), Bcl-2 (Dako, Kingsgrove, NSW, Australia), p-Rb^{T826} (Sigma-Aldrich), and p42/44 (Protein Simple, San Jose, CA). Both anti-mouse and anti-rabbit immunoglobulin G horseradish peroxidase–conjugated antibodies were obtained from Dako. Enhanced chemiluminescence reagents were obtained from GE Healthcare Life Sciences (Rydalmere, NSW, Australia).

Statistical Analyses. All experiments were performed in triplicate and repeated at least three times; representative experiments were selected for figures. The statistical significance of the differences observed between the experimental groups was determined using one-way analysis of variance with a minimal level of significance at $P < 0.05$.

Results

MNKI-19 and MNKI-85 Are Potent and Selective Mnk Inhibitors. The thienopyrimidinyl derivative MNKI-19 inhibits Mnk1 and Mnk2 potently with K_i values of 0.186 and 0.068 μM, respectively, by biochemical assays (Table 1). MNKI-85 exhibits ~2-fold increased inhibitory activity against Mnk2 (K_i = 0.031 μM) when compared with MNKI-19, but is completely inactive against Mnk1. No inhibitory activities against CDK2A, CDK9T, and CDK4D were detected with both compounds (K_i > 10 μM). To further profile kinase selectivity, MNKI-19 and MNKI-85 were tested against a panel of upstream activating kinases of Mnks, including B-Raf, MAPK1, MAPK2, Akt1, PI3K, p38α, and mTOR, at 5 μM (Fig. 1). FLT3 protein is an upstream affector of both the Ras/Raf/MAPK and PI3K/Akt/mTOR pathways (Wander et al., 2014). As one of the downstream effectors of FLT3, Pim-1 was inhibited potently by cercosporamide (Konicek

TABLE 1

Chemical structure and kinase inhibitory activity of Mnk inhibitors

The ATP concentrations used in these assays were within 15 μM of K_m. Apparent inhibition constants (K_i) were calculated from IC_{50} values and the appropriate K_m (ATP) values for each kinase using the Cheng-Prusoff equation. Data shown are the mean values derived from two replicates ± S.D.

Compound		K_i (μM)						
		Mnk1	Mnk2	CDK2A	CDK9T1	CDK4D1	FLT3	Pim-1
CGP57380	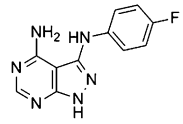 CGP57380	1.010 ± 0.098	0.877 ± 0.212	>10	>10	>10	ND	ND
MNKI-19	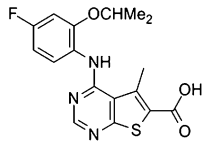 MNKI-19	0.186 ± 0.011	0.068 ± 0.009	>10	>10	>10	>10	2.35
MNKI-85	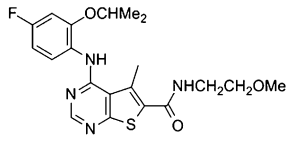 MNKI-85	>10	0.031 ± 0.012	>10	>10	>10	>10	>10

ND, not determined.

et al., 2011), thus it is of great interest to evaluate the inhibitory activities of the compounds against FLT3 and Pim-1. The results obtained from in-house immobilized metal ion affinity particle assays for Mnk1 and Mnk2 at 1 μM of the tested compounds were included for comparison. Both compounds are inactive against most of the upstream kinases, with the exception that MNKI-19 displays moderate activity against Pim-1 (K_i = 2.35 μM) (Table 1). However, it is 12- and 35-fold less active when compared with Mnk1 and Mnk2, respectively. Collectively, these data suggest the high specificity of MNKI-19 and MNKI-85 for Mnks.

MNKI-19 and MNKI-85 Exhibit Antileukemic Activity. The antiproliferative activity of both MNKI-19 and MNKI-85 was assessed on a panel of six AML cell lines and one chronic myeloid leukemia cell line (Table 2) using 72-hour resazurin assays. CGP57380 was included as a control. All compounds exhibited the greatest antiproliferative effects on MOLM-13 and MV4-11, both of which expressed FLT3-ITD (Quentmeier et al., 2003), with GI_{50} values ranging between 5.65 and 8.81 μM. In contrast, at least 4-fold higher concentrations of compounds MNKI-19 and MNKI-85 were required to suppress the proliferation of HL-60, K562, THP-1, and U937 [wild-type (WT) FLT3 expression]. Surprisingly, PL-21 cells, expressing both WT and mutated alleles, showed less sensitivity in response to the same treatments. Different antiproliferative effects on these cells have also been observed with CGP57380, which modestly suppressed cell proliferation with GI_{50} values ranging from 6.89 to 38.97 μM, suggesting an alternative mechanism underlying the growth inhibitory effects for CGP57380. Taken together, these data suggest that cellular effects of the Mnk inhibitors are more pronounced against AML cells with FLT3-ITD expression than the nonmutated FLT3 cells. It is worth noting that these thienopyrimidinyl derivatives also display cell-specific effects between cancerous and normal cells. The normal lung fibroblast WI-38 cells were insensitive to both MNKI-19 and MNKI-85 with GI_{50} values of 98.63 and 43.40 μM, respectively (Table 2).

MNKI-19 and MNKI-85 Inhibits the Phosphorylation of eIF4E and 4E-BP1. We next examined cellular Mnk inhibition of MNKI-19 and MNKI-85 by Western blot analysis (Fig. 2). MOLM-13 cells were treated with CGP57380, MNKI-19, or MNKI-85 at 5 and/or 10 and 20 μM for a period of 1 hour. As shown in Fig. 2A, both MNKI-19 and MNK-85 completely depleted the phosphorylation of eIF4E at Ser209 (p-eIF4E^{S209}) at a lower concentration (i.e., 5 μM), whereas CGP57380 moderately suppressed p-eIF4E^{S209} within the same concentration. These results confirm the cellular inhibition of Mnk and the relative potency of MNKI-19 and MNKI-85 against Mnks over CGP57380. The treatment caused no changes in the

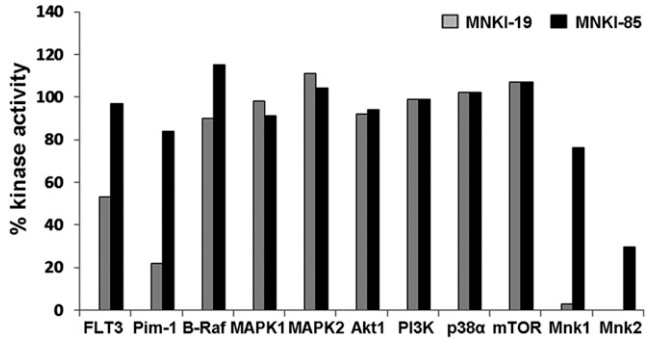

Fig. 1. Selectivity of MNKI-19 and MNKI-85 against a panel of kinases. The remaining percentages of kinase activity upon treatment with each compound at a concentration 5 μM are shown, unless otherwise specified. Both Mnk1 and Mnk2 are tested by the in-house immobilized metal ion affinity particle assays at 1 μM of compound inhibitors; 15 μM within K_m of ATP for each kinase is used in the assays. Data represent one repeat, and kinases that show <50% in kinase activity upon compound treatment are further evaluated with dose-response analysis to obtain their apparent inhibition constants (K_i) as shown in Table 1.

TABLE 2
Antiproliferative activity of CGP57380, MNKI-19, and MNKI-85 in leukemia cell lines with various FLT3 mutational statuses and normal fibroblast cells by 72-hour resazurin and MTT assays, respectively

Cell Line	FLT3 Status	FAB Subtype	72-hour GI_{50} (μM)[a] ± S.D.		
			CGP57380	MNKI-19	MNKI-85
MOLM-13	ITD	M5a	8.81 ± 0.80	5.65 ± 0.84	7.19 ± 0.08
MV4-11	ITD	M5	6.89 ± 0.16	7.30 ± 0.75	7.44 ± 0.77
PL-21	ITD/WT	M3	9.39 ± 0.11	57.17 ± 6.74	>100
HL-60	WT	M2	16.83 ± 1.98	69.18 ± 6.15	>100
THP-1	WT	M5	38.97 ± 2.98	>100	94.06 ± 8.40
U937	WT	M4/5	9.40 ± 0.60	33.59 ± 4.21	>100
K562	WT	(CML)	34.13 ± 1.82	93.16 ± 9.68	>100
WI-38[b]	Normal fibroblast cells	Normal fibroblast cells	62.37 ± 0.24	98.63 ± 1.54	43.40 ± 5.05

CML, chronic myeloid leukemia; FAB, French-American-British classification system.
[a]Data shown are the mean values derived from at least two replicates ± S.D.
[b]The GI_{50} values were determined by 72-hour MTT assay.

expression of total eIF4E, Mnk1, and Mnk2 proteins. To assess the Mnk-targeting specificity, the effects of MNKI-19 or MNKI-85 on the upstream activating kinases, including p38 MAPK, ERK, eIF4E-binding protein 1 (4E-BP1), and their phosphorylated forms, were analyzed in MOLM-13 cells. Incubation with MNKI-19 for 1 hour upregulated an early transient phosphorylation of ERK and p38 in a dose-dependent manner, without affecting their total levels. The expression levels of protein 4E-BP1 and its phosphorylated forms at Thr37/46 and Thr70 are not affected, which is consistent with the kinase assays showing no inhibitory activity against mTOR with MNKI-19 and MNKI-85 (Fig. 1). Similar effects were seen in CGP57380-treated cells but not in MNKI-85. However, little to no effect on the levels of p38 and ERK proteins and their phosphorylated forms was observed after treating MOLM-13 with 20 μM compounds for 24 hours (Fig. 2B). After 24 hours, the complete abolition of p-eIF4E^{S209} by Mnk inhibitors gave rise to a reduction in the phosphorylation of 4E-BP1 at Thr37/46 (Fig. 2C; Supplemental Fig. 1) and Thr70 (Fig. 2C), particularly at the latter in a dose-dependent manner, in MOLM-13 cells.

MNKI-19 and MNKI-85 Arrest Cancer Cells in the G_1 Phase of the Cell Cycle via Downregulation of CDK4 and Cyclin D3. We next investigated whether the antiproliferative activity of MNKI-19 and MNKI-85 was a consequence of cell cycle effects. As shown in Fig. 3A, treatment of MOLM-13 cells with MNKI-19 or MNKI-85 at 5 μM for 24 hours resulted in the accumulation of G_1 cells, which was accompanied by a loss in cell population at the G_2/M phase. This is consistent with previous studies (Zhang et al., 2008; Diab et al., 2014b). The cell cycle effect of MNKI-19 was found to behave in a dose- and time-dependent manner. Consistently, this was observed with MV4-11 cells after treatment with the compounds (Fig. 3B). However, in the case of MNKI-85 there was no significant change in the cell cycle distribution observed with longer treatment time. Time-course Western blot analysis was conducted to study the levels of key proteins involved in the cell cycle after treatment of MOLM-13 cells with compound inhibitors for 1 and 24 hours. Attempts were made to study the expression level of cyclin D1 in MOLM-13 cells but the protein was too weak to be detected (unpublished data), hence cyclin D3 was pursued. In human somatic cells, the G_1 to S phase transition is tightly regulated by the cyclin-D/CDK4/6 proteins, along with their downstream target, the Rb protein (Neganova and Lako, 2008). As shown in Fig. 3C, no significant changes were detected in these cell cycle regulators at the early time point (i.e., 1 hour) (see also Supplemental Fig. 2). However, 24-hour incubation of MOLM-13 cells with Mnk inhibitors resulted in the suppression of cyclin D3 expression in a dose-dependent manner (Fig. 3D). CDK4 was also downregulated by Mnk inhibitors at low concentrations.

To investigate whether the perturbation of cell cycle progression is a consequence of CDK4 activity, the phosphorylation of Rb at both CDK4-specific Thr826 (p-Rb^{T826}) sites (Macdonald and Dick, 2012) was also measured. A decreased level of p-Rb^{T826} was detected upon treatment of MOLM-13 cells with 20 μM of MNKI-19 or MNKI-85 (Fig. 3D; Supplemental Fig. 3), indicating the loss of CDK4 activity and restriction of the G_1 to S transition. This observation is further supported by kinase assays showing that both MNKI-19 and MNKI-85 have no inhibitory effect on CDK4 kinase activity (Table 1), implying the decreased CDK4 protein expression is a consequence of the downregulating Mnk/eIF4E-mediated protein synthesis of cyclin D3. In contrast, little effect on CDK6 or CDK6-specific p-Rb^{T821} levels was observed (Fig. 3E; Supplemental Fig. 4), supporting the relative importance of CDK4 over CDK6 in the cell cycle progression (Neganova and Lako, 2008).

MNKI-19 and MNKI-85 Induce Apoptosis in FLT3-ITD–Expressed AML Cells. The apoptotic mechanism of action by Mnk inhibitors was further examined using annexin V/PI staining. Exposure of MOLM-13 or MV4-11 cells to either MNKI-19, MNKI-85, or CGP57380 at a concentration of 10 or 20 μM for 24 hours caused a 2- to 4-fold increase in apoptotic cells (annexin V^+/PI^- and annexin V^+/PI^+) when compared with untreated cells (Fig. 4, A and B). Consistent with the cell cycle profile, MNKI-19 induced significant apoptosis in a dose- and time-dependent manner. While the proteins involved in the apoptosis mechanism, including Mcl-1, Bcl-2, PARP, and caspase-3, were not affected in MOLM-13 cells at the early time point (i.e., 1 hour) (Fig. 4C), Western blot analysis revealed the downregulation of the anti-apoptotic protein Mcl-1 and/or an increase of PARP cleavage after exposure to 5 μM of MNKI-19, MNKI-85, or CGP57380 for 24 hours (Fig. 4D), indicating the apoptotic effect caused by the inhibition of Mnks. The levels of Bcl-2 remain unchanged (Fig. 4E), which is in agreement with our previous results obtained using MV4-11 (Diab et al., 2014b).

In conjunction with no aberration in full-length caspase-3 protein levels (Fig. 4E) and no detectable caspase-3/7 activity (Fig. 4F), the data indicate that Mnk inhibitor-induced apoptosis in MOLM-13 and MV4-11 cells may be independent of caspases-3 and -7.

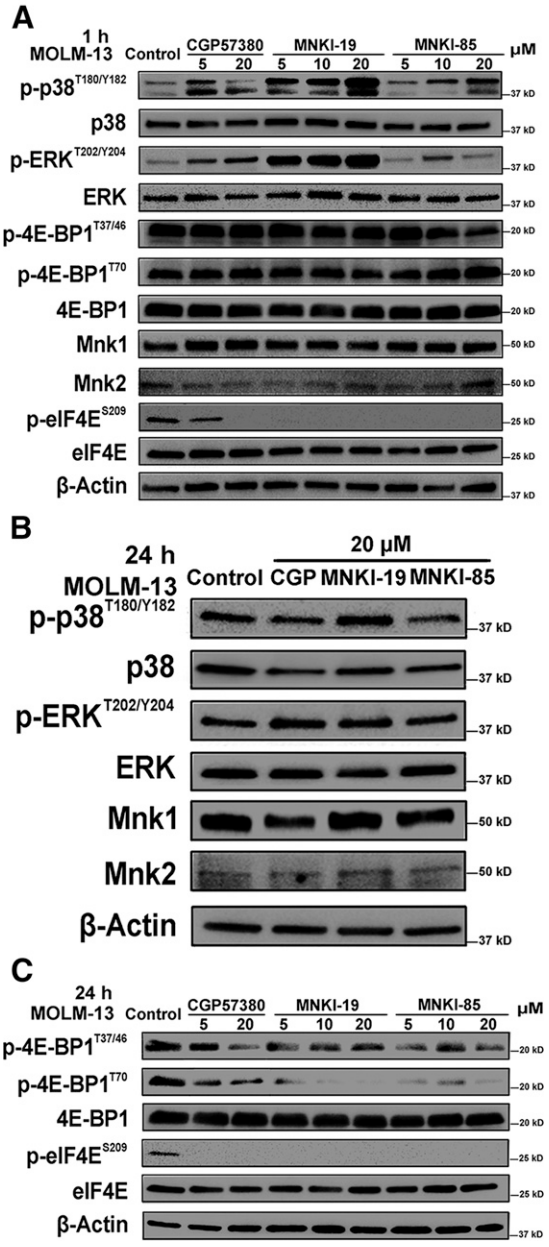

Fig. 2. Western blot analysis of key proteins involved in the Ras/Raf/MAPK and PI3K/Akt/mTOR pathways in MOLM-13 cells treated with CGP57380, MNKI-19, and MNKI-85 for (A) 1 hour and (B and C) 24 hours. In (A) and (C) compounds are tested at 5 and/or 10 and 20 μM, whereas in (B) compounds are used at 20 μM. Antibodies used and the protein molecular weight marker are indicated on the left and right sides of each panel, respectively. DMSO diluent is used as a control and β-actin is used as an internal loading control. A representative blot is selected from at least two independent repeats.

Discussion

Screening against a panel of seven leukemia cell lines with various FLT3 mutational statuses revealed that the selective Mnk inhibitors MNKI-19 and MNKI-85 are particularly effective in suppressing the growth of FLT3/ITD-expressing AML cells, including MOLM-13 and MV4-11. PL-21 cells, in contrast, expressing both WT and mutated alleles (Quentmeier et al., 2003), were less sensitive to these compounds. However, it remains debatable that PL-21 cells could only express the WT allele (Yokota et al., 1997). Nevertheless, the differences in the sensitivity between the cell lines could be attributed to the different subtypes, which are classified based on the morphology and immunohistochemistry of myeloid neoplasms (Bennett et al., 1985). Both MOLM-13 and MV4-11 are acute monoblastic leukemia cells (M5/M5a) (Quentmeier et al., 2003) that carry the respective t(9,11) and t(4,11) chromosomal translocations, resulting in the fusion proteins MLL-AF9 and MLL-AF4, respectively (Matsuo et al., 1997; Andersson et al., 2005). Of note, these subtypes of AML are correlated with aberrant upregulation of eIF4E (Topisirovic et al., 2003), which is absent in the less mature promyelocytic cells (M3; PL-21 cells) (Quentmeier et al., 2003). As a comparator, THP-1 cells with the t(9,11) chromosomal translocation and no detectable FLT3-ITD expression exhibited negligible sensitivity to MNKI-19 and MNKI-85 (>12-fold). Similarly, HL-60, U937, and K562, which do not express ITD mutations, have no cytotoxic effects when treated with the compounds for up to 3 days. These results are in agreement with a previous study, in which inhibiting 50% of cell growth in K562, U937, and MM6 cell lines after 5-day treatment also required >10 μM of cercosporamide (Altman et al., 2013). On the other hand, CGP57380 is not particularly selective against the ITD-positive cells, indicating an alternative mechanism underlying the growth inhibitory effects. When considered together, concurrently activated upstream signaling pathways of Mnks with overexpressed eIF4E levels, as characterized by the combined FLT3-ITD mutations and M5 subtypes, may serve as the right platform for investigation of the antileukemic effects of Mnk-specific inhibitors.

Western blot analysis further confirmed the role of MNKI-19 and MNKI-85 as potent Mnk inhibitors, as evidenced by the blockage of eIF4E^{S209} phosphorylation. Because Mnks are important convergence nodes of the MAPK pathways (Faivre et al., 2006; Chappell et al., 2011), the expression of the upstream effectors, p38 and ERK, was also investigated. Interestingly, an early transient phosphorylation of ERK and p38 was found to be upregulated upon incubation with MNKI-19 for 1 hour, without affecting their total levels. Similar effects were seen in CGP57380-treated cells but not in MNKI-85. This could be attributed to the induction of a negative-feedback mechanism upon Mnk1 inhibition since both ERK and p38 are substrates for Mnk1 (Waskiewicz et al., 1997). Such an observation is consistent with a study done by Zhang et al. (2008), who reported that CGP57380-mediated ERK and Mnk activation was determined at an early time point (i.e., 30 minutes) and followed by a second late phosphorylation starting at 24 hours in the Bcr-Abl–dependent cells. Little to no effect on the levels of ERK and p38 proteins and their phosphorylated forms was observed after treating MOLM-13 with 20 μM compounds for 24 hours, supporting the observation that the sustained phosphorylation at a late time point is dependent on the presence of Bcr-Abl and signifying the specific effect of our Mnk inhibitors on Mnk/eIF4E. The compounds were also evaluated against a panel of upstream activating kinases, including B-Raf, ERK, p38α, PI3K, Akt1, and mTOR, using biochemical assays, and showed no significant kinase inhibitory activity, supporting selectivity of the compounds.

Interestingly, downregulation of the levels of phosphorylated 4E-BP1 at Thr37/46 and Thr70 (the two most priming phosphorylation events for the upstream affector mTOR) (Gingras et al., 2001) were detected in MOLM-13 cells treated with either MNKI-19 or MNKI-85. Binding of eIF4E to 4E-BP1 is regulated by hierarchical multisite phosphorylation,

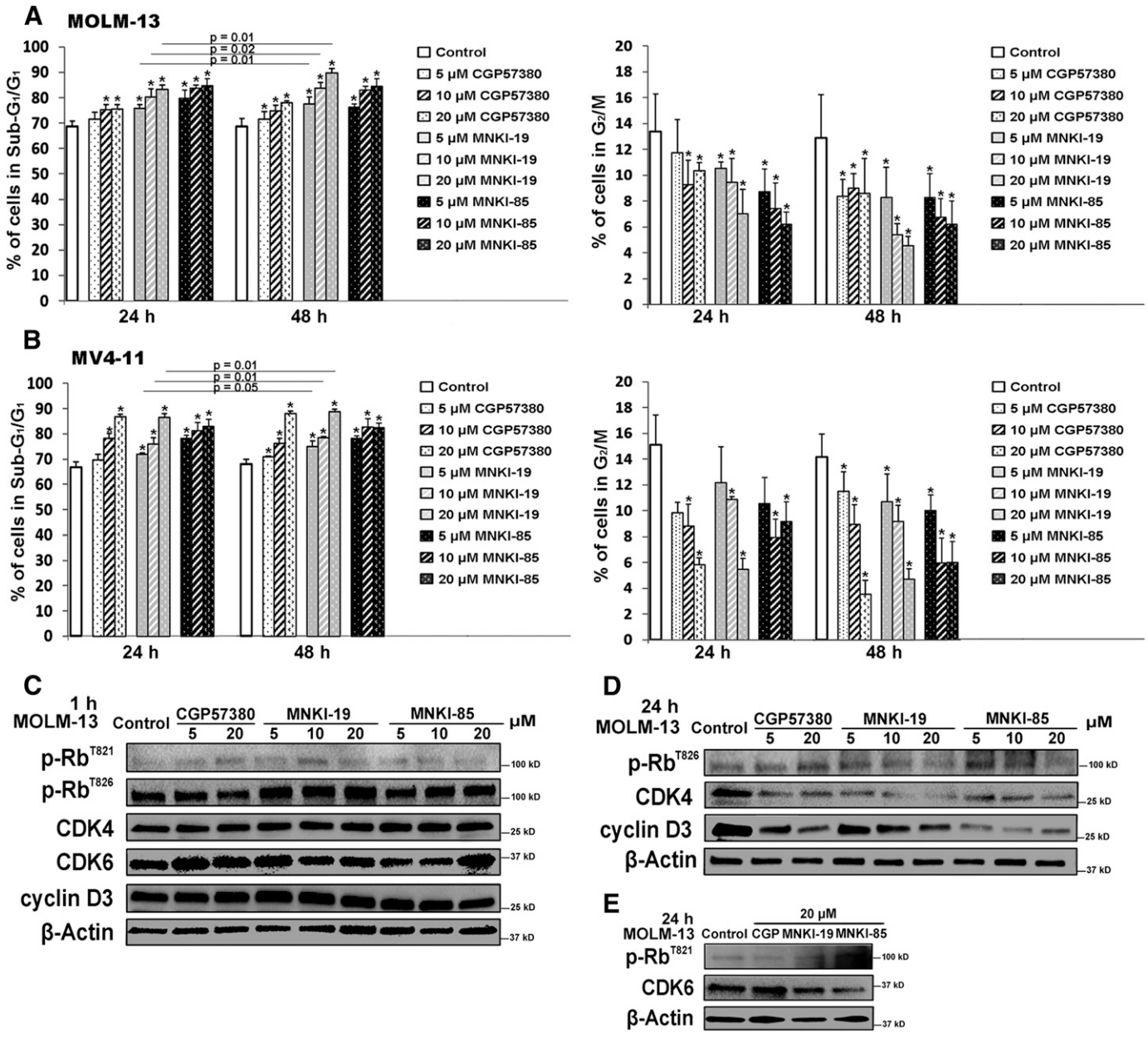

Fig. 3. Cell cycle analysis of (A) MOLM-13 and (B) MV4-11 cells after treatment with 5, 10, or 20 μM of MNKI-19, MNKI-85, or CGP57380 for 24 and 48 hours. Data represent the mean ± S.D. of three independent repeats. *$P < 0.05$ when compared with the control. Western blot analysis of key proteins involved in the cell cycle upon treatment with Mnk inhibitors in MOLM-13 cells for (C) 1 hour and (D and E) 24 hours. In (C) and (D) compounds are tested at 5 and/or 10 and 20 μM, whereas in (E) compounds are used at 20 μM. Antibodies used and the protein molecular weight marker are indicated on the left and right sides of each panel, respectively. DMSO diluent is used as a control and β-actin is used as an internal loading control. A representative blot is selected from at least two independent repeats.

and the role of the phosphorylation site at Thr37/46 on eIF4E binding remains controversial: several studies claimed that the phosphorylation of Thr37/46 has little effect on the binding of eIF4E (Gingras et al., 1999; Karim et al., 2001), while the other group showed that a significant reduction in eIF4E-binding affinity was induced by such a phosphorylation event (Burnett et al., 1998). However, mutations of these residues and/or Thr70 to alanine have significantly led to the dissociation of eIF4E from 4E-BP1 (Gingras et al., 2001), confirming the important role of these phosphorylation sites on the eIF4E/4E-BP1 equilibrium.

In light of these findings, it is speculated that a negative-feedback regulatory mechanism involving the equilibrium shift toward the eIF4E/4E-BP1 complex could be triggered in the compound-treated cells. Translation processes involve the assembly of several eIF4 translational factors, including the eIF4E and activated Mnks to form the eIF4F complex (Hou et al., 2012). Inhibition of Mnks, especially Mnk2, may increase the levels of eIF4E in the cells since the formation of eIF4F complex has been disrupted. Because the Akt/mTOR pathway is overly activated in FLT3-ITD MOLM-13 cells (Hayakawa et al., 2000), it is suspected that the upregulated eIF4E levels have initiated the negative-feedback mechanism of Akt/mTOR to dephosphorylate 4E-BP1. Upon hypo-phosphorylation, 4E-BP1 interacts strongly with eIF4E (Khaleghpour et al., 1999). While our compounds were inactive to the upstream kinases in the Akt/mTOR pathway, particularly mTOR, it is believed that

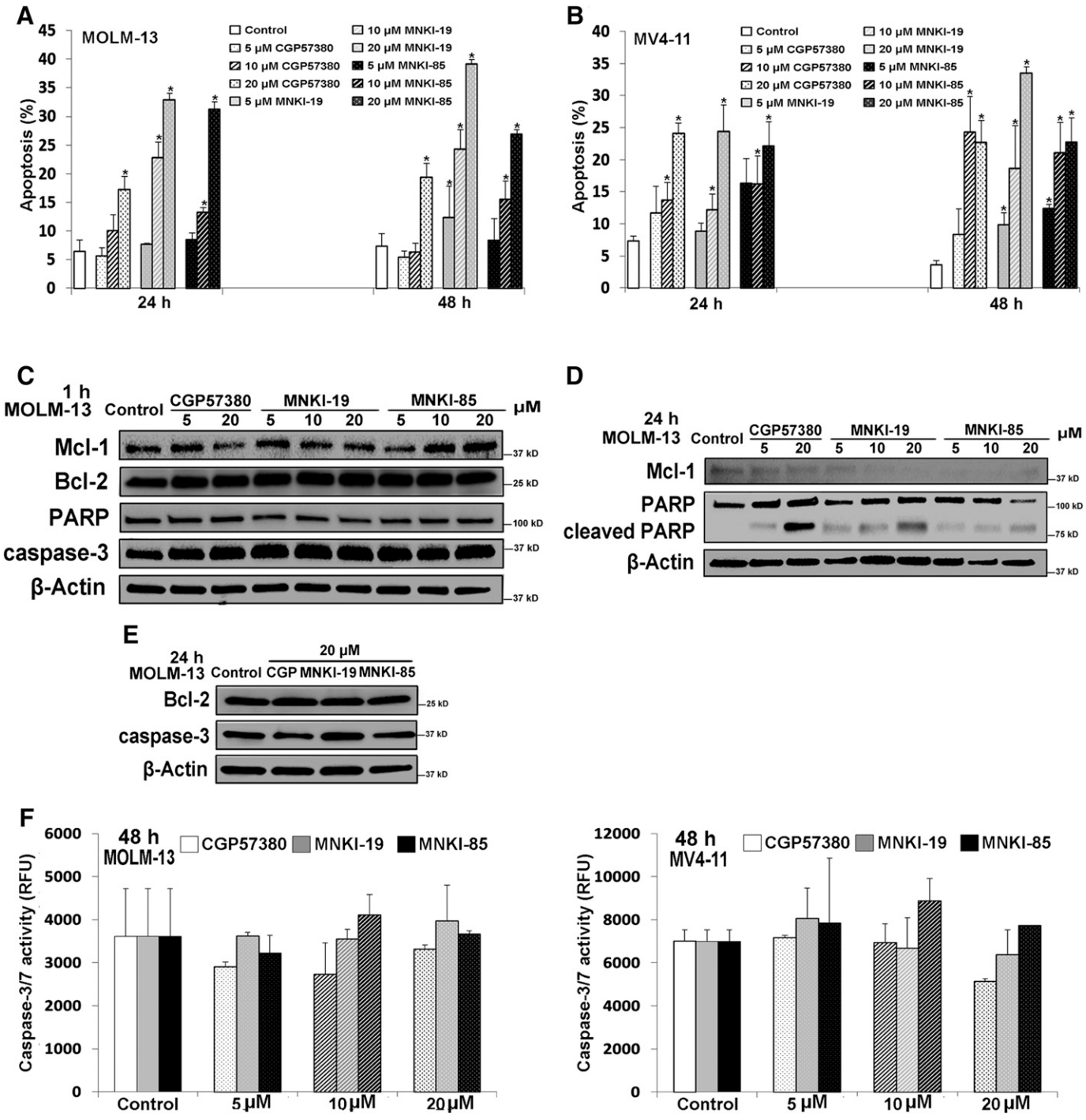

Fig. 4. Induction of apoptosis by MNKI-19, MNKI-85, or CGP57380 in (A) MOLM-13 and (B) MV4-11 cells. Cells are exposed at 5, 10, and 20 μM of each compound for 24 and 48 hours, and examined with Annexin V/PI staining. The percentage of cells undergoing apoptosis is represented by the sum of the early and late apoptosis. Data represent the mean ± S.D. of three independent repeats. $^*P < 0.05$ when compared with the control. Western blot analysis of key proteins involved in apoptosis upon treatment with Mnk inhibitors in MOLM-13 cells for (C) 1 hour and (D and E) 24 hours. In (C) and (D) compounds are tested at 5 and/or 10 and 20 μM, whereas in (E) compounds are used at 20 μM. Antibodies used and the protein molecular weight marker are indicated on the left and right sides of each panel, respectively. DMSO diluent is used as a control and β-actin is used as an internal loading control. A representative blot is selected from at least two independent repeats. (F) Quantification of caspase-3/7 activity in MOLM-13 (left) and MV4-11 (right) cells upon treatment with 5, 10, and 20 μM of MNKI-19, MNKI-85, or CGP57380 for 48 hours.

the dephosphorylation events were induced upon Mnk inhibition.

Complementary to this, a recent study used CGP57380 to investigate the effect of eIF4E phosphorylation on translation initiation, showing that the amount of eIF4G in the eIF4F complex was decreased when treated with the compound (Li et al., 2010). This implies that inhibiting Mnks may reduce the eIF4F assembly. Another recent study also suggested that the dissociation of 4E-BP1 is highly dependent on the Mnk1-mediated eIF4E phosphorylation (Das et al., 2013). The

dephosphorylation of 4E-BP1 by MNKI-19 could be also due to the Pim-1 inhibition as shown in the kinase assay. 4E-BP1 has recently been identified as a target of Pim-1 in the FLT3-ITD–driven activation of STAT-5. Pim-1 inhibitors have significantly reduced p-4E-BP1$^{T37/46}$ in FLT3-ITD AML cells (Chen et al., 2011). However, more studies on the binding affinity of compounds MNKI-19 and MNKI-85 for the relevant proteins, such as eIF4G and 4E-BP1, are required to unveil the underlying mechanism.

The oncogenic role of eIF4E has been reported in the cell cycle progression (Diab et al., 2014a). D-type cyclins, as G_1 progression factors, play a vital role in enhancing the G_1 to S transition through binding to CDK4/6 (Sherr, 1995). Elevated eIF4E levels have been shown to enhance the translational levels of a wide array of malignancy-related mRNAs involved in the regulation of cell senescence, proliferation, and apoptosis, including cyclin D1 and Mcl-1 (Zimmer et al., 2000), whereas the oncogenic functions of eIF4E are closely linked to its phosphorylation by Mnks (Ueda et al., 2010; Diab et al., 2014a). Consistent with previous studies (Zhang et al., 2008; Diab et al., 2014b; Teo et al., 2015), Mnk inhibitors in the current study triggered a cell cycle arrest in both MOLM-13 and MV4-11 cells by disrupting the transition of the G_1 phase to the S phase. Such an effect is likely to be the result of decreased expression of the key cell cycle regulators, including CDK4 and cyclin D3, which further hampered the phosphorylation of Rb at the CDK4-specific Thr826 site (Macdonald and Dick, 2012). This was further supported when kinase assays showed both MNKI-19 and MNKI-85 have no effect on CDK4 kinase activity ($K_i > 10$ μM). Previous studies also demonstrated the importance of cyclin D3 at the translational level over other D-type cyclins (Prabhu et al., 2007; Zhang et al., 2008).

Collectively, these results indicate that the effect of eIF4E-mediated cell cycle arrest is through phosphorylation by Mnks. While MNKI-19 increased the G_1 cell accumulation in a time-dependent manner, MNKI-85 failed to show a similar cell cycle effect, suggesting that targeting a combination of Mnk1 and Mnk2 may be more effective than one of the isoforms alone in preventing cell cycle progression. Our observation agrees with a recent study on a series of Mnk degrading agents, which showed they induce G_1/G_0 cell cycle arrest, along with the downregulation of cyclin D3 and CDK4 in MDA-MB-231 cells (Ramalingam et al., 2014).

The apoptotic effect of Mnk inhibitors is likely mediated through the 4E-BP1/eIF4E axis. Several lines of evidence have indicated the positive correlation between the suppression of eIF4E by binding to 4E-BP1 and induction of apoptosis (Clemens, 2001; Yellen et al., 2013). To date, Mnk1 and Mnk2 are the only identified kinases that phosphorylate eIF4E, and phosphorylation of eIF4E modulates cap-dependent translation. In addition, eIF4E phosphorylation can be downregulated by 4E-BP1 binding (Li et al., 2010); therefore, this has raised the possibility that inhibiting Mnks triggers the dephosphorylation of 4E-BP1 and results in the reduction of cap-dependent protein synthesis, including Mcl-1. In contrast, the significant induction of G_1 arrest and apoptosis by MNKI-19 could also be an additive effect of Pim-1 inhibition. A previous study has shown that Pim-1 inhibitors reduced Mcl-1 and induced apoptosis in FLT3-ITD AML cells (Chen et al., 2011).

We have shown that inhibition of eIF4E phosphorylation with Mnk inhibitors is associated with an increase in cell death. An increase cleavage of PARP and a marked suppression of Mcl-1 levels were observed. Lack of procaspase-3 processing and caspase-3/7 activation suggest that the apoptotic cell death by Mnk inhibitors may be via a caspase-independent mechanism. In contrast, a recent study demonstrated a caspase-dependent apoptosis was induced with Mnk degrading agents in breast cancer cell lines (Ramalingam et al., 2014). Perhaps modes of action are contingent on compounds treated and cell lines tested. However, it is noteworthy that a combined use of Mnk1 and Mnk2, as represented by MNKI-19, gives rise to a more pronounced apoptosis than inhibiting Mnk2 alone (MNKI-85).

Acknowledgments

The authors thank Professor Richard D'Andrea (University of South Australia) for the generous supply of the AML cell lines.

Authorship Contributions

Participated in research design: Wang, Teo.
Conducted experiments: Teo, Basnet.
Contributed new reagents or analytic tools: Yang, Yu.
Performed data analysis: Teo, Lam, Basnet, Albrecht, Wang.
Wrote or contributed to the writing of the manuscript: Teo, Wang, Yu, Sykes.

References

Altman JK, Szilard A, Konicek BW, Iversen PW, Kroczynska B, Glaser H, Sassano A, Vakana E, Graff JR, and Platanias LC (2013) Inhibition of Mnk kinase activity by cercosporamide and suppressive effects on acute myeloid leukemia precursors. *Blood* **121:**3675–3681.

Andersson A, Edén P, Lindgren D, Nilsson J, Lassen C, Heldrup J, Fontes M, Borg A, Mitelman F, and Johansson B et al. (2005) Gene expression profiling of leukemic cell lines reveals conserved molecular signatures among subtypes with specific genetic aberrations. *Leukemia* **19:**1042–1050.

Bennett JM, Catovsky D, Daniel MT, Flandrin G, Galton DA, Gralnick HR, and Sultan C (1985) Proposed revised criteria for the classification of acute myeloid leukemia. A report of the French-American-British Cooperative Group. *Ann Intern Med* **103:**620–625.

Burnett PE, Barrow RK, Cohen NA, Snyder SH, and Sabatini DM (1998) RAFT1 phosphorylation of the translational regulators p70 S6 kinase and 4E-BP1. *Proc Natl Acad Sci USA* **95:**1432–1437.

Chappell WH, Steelman LS, Long JM, Kempf RC, Abrams SL, Franklin RA, Bäsecke J, Stivala F, Donia M, and Fagone P et al. (2011) Ras/Raf/MEK/ERK and PI3K/PTEN/Akt/mTOR inhibitors: rationale and importance to inhibiting these pathways in human health. *Oncotarget* **2:**135–164.

Chen LS, Redkar S, Taverna P, Cortes JE, and Gandhi V (2011) Mechanisms of cytotoxicity to Pim kinase inhibitor, SGI-1776, in acute myeloid leukemia. *Blood* **118:**693–702.

Cheng Y and Prusoff WH (1973) Relationship between the inhibition constant (K1) and the concentration of inhibitor which causes 50 per cent inhibition (I50) of an enzymatic reaction. *Biochem Pharmacol* **22:**3099–3108.

Clemens MJ (2001) Translational regulation in cell stress and apoptosis. Roles of the eIF4E binding proteins. *J Cell Mol Med* **5:**221–239.

Das F, Ghosh-Choudhury N, Bera A, Kasinath BS, and Choudhury GG (2013) TGFβ-induced PI3 kinase-dependent Mnk-1 activation is necessary for Ser-209 phosphorylation of eIF4E and mesangial cell hypertrophy. *J Cell Physiol* **228:**1617–1626.

Dash A and Gilliland DG (2001) Molecular genetics of acute myeloid leukaemia. *Best Pract Res Clin Haematol* **14:**49–64.

Diab S, Kumarasiri M, Yu M, Teo T, Proud C, Milne R, and Wang S (2014a) MAP kinase-interacting kinases—emerging targets against cancer. *Chem Biol* **21:** 441–452.

Diab S, Teo T, Kumarasiri M, Li P, Yu M, Lam F, Basnet SK, Sykes MJ, Albrecht H, and Milne R et al. (2014b) Discovery of 5-(2-(phenylamino)pyrimidin-4-yl)thiazol-2(3H)-one derivatives as potent Mnk2 inhibitors: synthesis, SAR analysis and biological evaluation. *ChemMedChem* **9:**962–972.

Faivre S, Djelloul S, and Raymond E (2006) New paradigms in anticancer therapy: targeting multiple signaling pathways with kinase inhibitors. *Semin Oncol* **33:** 407–420.

Furic L, Rong L, Larsson O, Koumakpayi IH, Yoshida K, Brueschke A, Petroulakis E, Robichaud N, Pollak M, and Gaboury LA et al. (2010) eIF4E phosphorylation promotes tumorigenesis and is associated with prostate cancer progression. *Proc Natl Acad Sci USA* **107:**14134–14139.

Gilliland DG and Griffin JD (2002) Role of FLT3 in leukemia. *Curr Opin Hematol* **9:** 274–281.

Gilliland DG, Jordan CT, and Felix CA (2004) The molecular basis of leukemia. *Hematology Am Soc Hematol Educ Program* **2004:**80–97.

Gingras AC, Gygi SP, Raught B, Polakiewicz RD, Abraham RT, Hoekstra MF, Aebersold R, and Sonenberg N (1999) Regulation of 4E-BP1 phosphorylation: a novel two-step mechanism. *Genes Dev* **13:**1422–1437.

Gingras AC, Raught B, Gygi SP, Niedzwiecka A, Miron M, Burley SK, Polakiewicz RD, Wyslouch-Cieszynska A, Aebersold R, and Sonenberg N (2001) Hierarchical phosphorylation of the translation inhibitor 4E-BP1. *Genes Dev* **15:**2852–2864.

Hanada M, Feng J, and Hemmings BA (2004) Structure, regulation and function of PKB/AKT—a major therapeutic target. *Biochim Biophys Acta* **1697:**3–16.
Hayakawa F, Towatari M, Kiyoi H, Tanimoto M, Kitamura T, Saito H, and Naoe T (2000) Tandem-duplicated Flt3 constitutively activates STAT5 and MAP kinase and introduces autonomous cell growth in IL-3-dependent cell lines. *Oncogene* **19:**624–631.
He LZ, Tribioli C, Rivi R, Peruzzi D, Pelicci PG, Soares V, Cattoretti G, and Pandolfi PP (1997) Acute leukemia with promyelocytic features in PML/RARα transgenic mice. *Proc Natl Acad Sci USA* **94:**5302–5307.
Hou J, Lam F, Proud C, and Wang S (2012) Targeting Mnks for cancer therapy. *Oncotarget* **3:**118–131.
Karim MM, Hughes JM, Warwicker J, Scheper GC, Proud CG, and McCarthy JE (2001) A quantitative molecular model for modulation of mammalian translation by the eIF4E-binding protein 1. *J Biol Chem* **276:**20750–20757.
Khaleghpour K, Pyronnet S, Gingras AC, and Sonenberg N (1999) Translational homeostasis: eukaryotic translation initiation factor 4E control of 4E-binding protein 1 and p70 S6 kinase activities. *Mol Cell Biol* **19:**4302–4310.
Konicek BW, Stephens JR, McNulty AM, Robichaud N, Peery RB, Dumstorf CA, Dowless MS, Iversen PW, Parsons S, and Ellis KE et al. (2011) Therapeutic inhibition of MAP kinase interacting kinase blocks eukaryotic initiation factor 4E phosphorylation and suppresses outgrowth of experimental lung metastases. *Cancer Res* **71:**1849–1857.
Lewis TS, Shapiro PS, and Ahn NG (1998) Signal transduction through MAP kinase cascades. *Adv Cancer Res* **74:**49–139.
Li Y, Yue P, Deng X, Ueda T, Fukunaga R, Khuri FR, and Sun SY (2010) Protein phosphatase 2A negatively regulates eukaryotic initiation factor 4E phosphorylation and eIF4F assembly through direct dephosphorylation of Mnk and eIF4E. *Neoplasia* **12:**848–855.
Lim S, Saw TY, Zhang M, Janes MR, Nacro K, Hill J, Lim AQ, Chang CT, Fruman DA, and Rizzieri DA et al. (2013) Targeting of the MNK-eIF4E axis in blast crisis chronic myeloid leukemia inhibits leukemia stem cell function. *Proc Natl Acad Sci USA* **110:**E2298–E2307.
Macdonald JI and Dick FA (2012) Posttranslational modifications of the retinoblastoma tumor suppressor protein as determinants of function. *Genes Cancer* **3:**619–633.
Martelli AM, Nyåkern M, Tabellini G, Bortul R, Tazzari PL, Evangelisti C, and Cocco L (2006) Phosphoinositide 3-kinase/Akt signaling pathway and its therapeutical implications for human acute myeloid leukemia. *Leukemia* **20:**911–928.
Matsuo Y, MacLeod RA, Uphoff CC, Drexler HG, Nishizaki C, Katayama Y, Kimura G, Fujii N, Omoto E, and Harada M et al. (1997) Two acute monocytic leukemia (AML-M5a) cell lines (MOLM-13 and MOLM-14) with interclonal phenotypic heterogeneity showing MLL-AF9 fusion resulting from an occult chromosome insertion, ins(11;9)(q23;p22p23). *Leukemia* **11:**1469–1477.
Meshinchi S, Woods WG, Stirewalt DL, Sweetser DA, Buckley JD, Tjoa TK, Bernstein ID, and Radich JP (2001) Prevalence and prognostic significance of Flt3 internal tandem duplication in pediatric acute myeloid leukemia. *Blood* **97:**89–94.
Milella M, Kornblau SM, Estrov Z, Carter BZ, Lapillonne H, Harris D, Konopleva M, Zhao S, Estey E, and Andreeff M (2001) Therapeutic targeting of the MEK/MAPK signal transduction module in acute myeloid leukemia. *J Clin Invest* **108:**851–859.
Neganova I and Lako M (2008) G1 to S phase cell cycle transition in somatic and embryonic stem cells. *J Anat* **213:**30–44.
Parra JL, Buxadé M, and Proud CG (2005) Features of the catalytic domains and C termini of the MAPK signal-integrating kinases Mnk1 and Mnk2 determine their differing activities and regulatory properties. *J Biol Chem* **280:**37623–37633.
Prabhu S, Saadat D, Zhang M, Halbur L, Fruehauf JP, and Ong ST (2007) A novel mechanism for Bcr-Abl action: Bcr-Abl-mediated induction of the eIF4F translation initiation complex and mRNA translation. *Oncogene* **26:**1188–1200.
Quentmeier H, Reinhardt J, Zaborski M, and Drexler HG (2003) FLT3 mutations in acute myeloid leukemia cell lines. *Leukemia* **17:**120–124.
Ramalingam S, Gediya L, Kwegyir-Afful AK, Ramamurthy VP, Purushottamachar P, Mbatia H, and Njar VC (2014) First MNKs degrading agents block phosphorylation of eIF4E, induce apoptosis, inhibit cell growth, migration and invasion in triple negative and Her2-overexpressing breast cancer cell lines. *Oncotarget* **5:**530–543.
Roux PP and Blenis J (2004) ERK and p38 MAPK-activated protein kinases: a family of protein kinases with diverse biological functions. *Microbiol Mol Biol Rev* **68:**320–344.
Scheper GC, Morrice NA, Kleijn M, and Proud CG (2001) The mitogen-activated protein kinase signal-integrating kinase Mnk2 is a eukaryotic initiation factor 4E kinase with high levels of basal activity in mammalian cells. *Mol Cell Biol* **21:**743–754.
Scheper GC, Parra JL, Wilson M, Van Kollenburg B, Vertegaal AC, Han ZG, and Proud CG (2003) The N and C termini of the splice variants of the human mitogen-activated protein kinase-interacting kinase Mnk2 determine activity and localization. *Mol Cell Biol* **23:**5692–5705.
Sherr CJ (1995) D-type cyclins. *Trends Biochem Sci* **20:**187–190.
Slentz-Kesler K, Moore JT, Lombard M, Zhang J, Hollingsworth R, and Weiner MP (2000) Identification of the human Mnk2 gene (MKNK2) through protein interaction with estrogen receptor beta. *Genomics* **69:**63–71.
Teo T, Yu M, Yang Y, Gillam T, Lam F, Sykes MJ, and Wang S (2015) Pharmacologic co-inhibition of Mnks and mTORC1 synergistically suppresses proliferation and perturbs cell cycle progression in blast crisis-chronic myeloid leukemia cells. *Cancer Lett* **357:**612–623.
Topisirovic I, Guzman ML, McConnell MJ, Licht JD, Culjkovic B, Neering SJ, Jordan CT, and Borden KL (2003) Aberrant eukaryotic translation initiation factor 4E-dependent mRNA transport impedes hematopoietic differentiation and contributes to leukemogenesis. *Mol Cell Biol* **23:**8992–9002.
Topisirovic I, Ruiz-Gutierrez M, and Borden KL (2004) Phosphorylation of the eukaryotic translation initiation factor eIF4E contributes to its transformation and mRNA transport activities. *Cancer Res* **64:**8639–8642.
Ueda T, Sasaki M, Elia AJ, Chio IIC, Hamada K, Fukunaga R, and Mak TW (2010) Combined deficiency for MAP kinase-interacting kinase 1 and 2 (Mnk1 and Mnk2) delays tumor development. *Proc Natl Acad Sci USA* **107:**13984–13990.
Ueda T, Watanabe-Fukunaga R, Fukuyama H, Nagata S, and Fukunaga R (2004) Mnk2 and Mnk1 are essential for constitutive and inducible phosphorylation of eukaryotic initiation factor 4E but not for cell growth or development. *Mol Cell Biol* **24:**6539–6549.
Wander SA, Levis MJ, and Fathi AT (2014) The evolving role of FLT3 inhibitors in acute myeloid leukemia: quizartinib and beyond. *Ther Adv Hematol* **5:**65–77.
Wang S, Wood G, Meades C, Griffiths G, Midgley C, McNae I, McInnes C, Anderson S, Jackson W, and Mezna M et al. (2004) Synthesis and biological activity of 2-anilino-4-(1H-pyrrol-3-yl) pyrimidine CDK inhibitors. *Bioorg Med Chem Lett* **14:**4237–4240.
Waskiewicz AJ, Flynn A, Proud CG, and Cooper JA (1997) Mitogen-activated protein kinases activate the serine/threonine kinases Mnk1 and Mnk2. *EMBO J* **16:**1909–1920.
Wendel HG, Silva RLA, Malina A, Mills JR, Zhu H, Ueda T, Watanabe-Fukunaga R, Fukunaga R, Teruya-Feldstein J, and Pelletier J et al. (2007) Dissecting eIF4E action in tumorigenesis. *Genes Dev* **21:**3232–3237.
Yellen P, Chatterjee A, Preda A, and Foster DA (2013) Inhibition of S6 kinase suppresses the apoptotic effect of eIF4E ablation by inducing TGF-β-dependent G1 cell cycle arrest. *Cancer Lett* **333:**239–243.
Yokota S, Kiyoi H, Nakao M, Iwai T, Misawa S, Okuda T, Sonoda Y, Abe T, Kahsima K, and Matsuo Y et al. (1997) Internal tandem duplication of the FLT3 gene is preferentially seen in acute myeloid leukemia and myelodysplastic syndrome among various hematological malignancies. A study on a large series of patients and cell lines. *Leukemia* **11:**1605–1609.
Yuan Y, Zhou L, Miyamoto T, Iwasaki H, Harakawa N, Hetherington CJ, Burel SA, Lagasse E, Weissman IL, and Akashi K et al. (2001) AML1-ETO expression is directly involved in the development of acute myeloid leukemia in the presence of additional mutations. *Proc Natl Acad Sci USA* **98:**10398–10403.
Zhang M, Fu W, Prabhu S, Moore JC, Ko J, Kim JW, Druker BJ, Trapp V, Fruehauf J, and Gram H et al. (2008) Inhibition of polysome assembly enhances imatinib activity against chronic myelogenous leukemia and overcomes imatinib resistance. *Mol Cell Biol* **28:**6496–6509.
Zimmer SG, DeBenedetti A, and Graff JR (2000) Translational control of malignancy: the mRNA cap-binding protein, eIF-4E, as a central regulator of tumor formation, growth, invasion and metastasis. *Anticancer Res* **20** (Suppl 3A)**:**1343–1351.

Address correspondence to: Shudong Wang, Centre for Drug Discovery and Development, School of Pharmacy and Medical Sciences, University of South Australia, Adelaide, South Australia 5001, Australia. E-mail: shudong.wang@unisa.edu.au